UCI-TR-2011-29, UH511-1182-11

New Constraints on Isospin-Violating Dark Matter

Jason Kumar,[1] David Sanford,[2] and Louis E. Strigari[3]

[1]*Department of Physics and Astronomy, University of Hawaii, Honolulu, HI 96822, USA*
[2]*Department of Physics and Astronomy, University of California, Irvine, CA 92697, USA*
[3]*Kavli Institute for Particle Astrophysics and Cosmology, Stanford University, Stanford, CA 94305 USA*

(Dated: December 2011)

We derive bounds on the dark matter annihilation cross-section for low-mass ($5-20$ GeV) dark matter annihilating primarily to up or down quarks, using the Fermi-LAT bound on gamma-rays from Milky Way satellites. For models in which dark matter-Standard Model interactions are mediated by particular contact operators, we show that these bounds can be directly translated into bounds on the dark matter-proton scattering cross-section. For isospin-violating dark matter, these constraints are tight enough to begin to constrain the parameter-space consistent with experimental signals of low-mass dark matter. We discuss possible models that can evade these bounds.

PACS numbers: 95.35.+d, 95.55.Ka

Introduction. There has been great interest in low-mass dark matter ($m_X \sim 5-20$ GeV) as a possible way to explain potential signals from the DAMA [1], CoGeNT [2] and CRESST [3] experiments. However, this data seems to be in tension with exclusion bounds from XENON10 [4], XENON100 [5], CDMS [6, 7] and SIMPLE [8]. Of these, the constraints from the xenon-based experiments appear to be the tightest. Attention has thus turned to new models which can potentially reconcile this data. One focus has been on isospin-violating dark matter (IVDM) [9–15], in which dark matter interactions between protons and neutrons are different. Although further reconciliation is required for complete consistency [16], destructive interference between dark matter couplings to protons and to neutrons can potentially relieve the tension between the CoGeNT, DAMA and XENON10/100 data sets. IVDM may thus play an important role in understanding the low-mass data.

A consequence of destructive interference is that the coupling of dark matter to up- and down-quarks must be relatively large for a given value of the dark matter-nucleus spin-independent scattering cross-section. This translates into larger annihilation and production cross-sections. Indirect detection and collider searches, where destructive interference plays no role, can thus provide stronger constraints on such dark matter models. In particular, the large annihilation cross-sections can enhance photon signals from the decays of hadrons produced in dark matter annihilation to up- and down-quarks. Because of their sensitivity to dark matter with mass in the range $\sim 5-20$ GeV, gamma-ray searches of dwarf spheroidal galaxies [17–19] can constrain these models.

In this Letter, we determine the constraints on the dark matter annihilation cross-section arising from gamma-ray searches of dwarf spheroidals, assuming dark matter annihilates entirely to up or down quarks. We then apply these constraints to IVDM models. We will see that if isospin-violation is the key feature in alleviating the tension between the DAMA, CoGeNT and XENON10/100 data sets, then models with purely contact interactions are tightly constrained by Fermi-LAT data. We also discuss how constraints on IVDM models weaken when dark matter-quark interactions occur through a light mediator.

Bounds from dwarf spheroidals. In [18], bounds on the dark matter annihilation cross-section were determined from a combined analysis of gamma-rays from dwarf spheroidals. This analysis compared the observed number of high-energy photons arriving directly from the dwarf spheroidals to the observed background slightly off-axis from the dwarf spheroidal. These bounds were expressed in terms of the quantity Φ_{PP}, defined as

$$\Phi_{PP} = \frac{\langle \sigma_A v \rangle}{8\pi m_X^2} \int_{E_{thr}}^{m_X} \sum_f B_f \frac{dN_f}{dE} dE, \qquad (1)$$

where B_f is the branching ratio for dark matter to annihilate to channel f. dN_f/dE is the photon spectrum for each annihilation channel and E_{thr} is the detector's threshold photon energy. Using $E_{thr} = 1$ GeV, [18] found the 95% CL bound

$$\Phi_{PP} \leq 5.0^{+4.3}_{-4.5} \times 10^{-30} \text{ cm}^3 \text{ s}^{-1} \text{ GeV}^{-2}, \qquad (2)$$

where the asymmetric uncertainties are 95% CL systematic errors [17], resulting from uncertainty in the mass density profile of the various satellites. 95% CL exclusion contours on the dark matter annihilation cross-section can thus be determined from eqs. 1,2 for any m_X, using the integrated photon distribution from each annihilation channel.

For annihilation to up or down quarks, we generated the photon spectrum using Pythia 6.409 [20], run on the computing cluster at the Hawaii Open Supercomputing Center. The up and down quark channels produce more photons than the τ-channel, resulting in tighter bounds. The bound for the $u\bar{u}$ channel is plotted in figure 1; the bound for the $d\bar{d}$ channel is slightly tighter than that for the $u\bar{u}$ channel, but the difference is never more than a percent for the given mass range. For these bounds, we

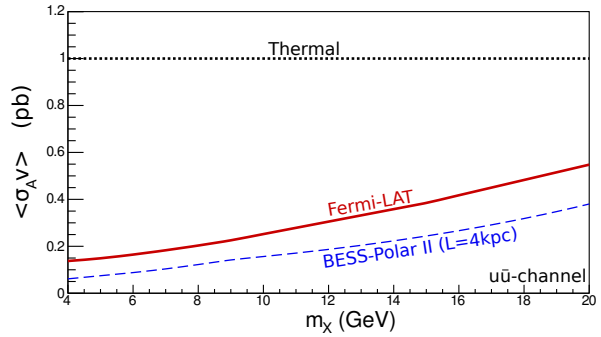

FIG. 1. 95% CL exclusion bound (see text) from Fermi in the $(m_X, \langle\sigma_A v\rangle)$ plane, assuming dark matter annihilation to $u\bar{u}$. The results for annihilation to the $d\bar{d}$ channel are visually identical. Also shown is the exclusion contour from BESS-Polar II for the same channel (assuming a diffusion halo size of 4 kpc). The dotted line indicates 1 pb, which is approximately the total annihilation cross-section at freeze-out for dark matter produced thermally in the early universe.

have assumed the central value of $\Phi_{PP} \leq 5.0$, applicable for the satellite mass density profiles found in [17]; allowing this to vary within 95% systematic error bars could weaken this bound by a factor of up to ~ 1.9, or strengthen it by a factor of up to ~ 10.

Dark matter annihilation to up- and down-quarks can also be constrained by limits on the cosmic ray anti-proton flux from experiments such as BESS-Polar II [21] and Pamela [22, 23]. Of these two experiments, BESS-Polar II reports tighter bounds, which we have plotted in figure 1 (light blue dashed curve, assuming a diffusion halo size of 4 kpc). The reported BESS-Polar II bound on dark matter annihilation to up- or down-quarks is tighter than the Fermi-LAT bound, given the astrophysics assumptions underlying both analyses. However, there are significant systematic astrophysical uncertainties which can weaken the anti-proton flux limits by up to a factor ~ 50 [24]. These include uncertainties regarding the background and the dark matter density profile of the galaxy, as well as uncertainties in the cosmic ray propagation model. Solar modulation can also sensitively affect bounds on dark matter annihilation arising from anti-proton flux measurements. Depending on these systematic uncertainties, the constraints on dark matter annihilation from the anti-proton flux may be weaker than those from gamma-ray searches of dwarf spheroidals.

The anti-proton flux uncertainties which we have discussed above are largely independent of the systematic uncertainties for gamma-rays from dwarf spheroidals, which derive primarily from the dark matter distribution within the spheroidal. These two indirect detection methods are thus quite complementary.

IVDM. We now apply these constraints to models of isospin-violating dark matter. We will consider the case in which dark matter interactions with Standard Model particles (both scattering and annihilation) are mediated by effective contact operators. The most general such effective operator can be written in terms of dark matter and quark bilinears, each of which transforms as either a scalar, pseudoscalar, vector, pseudovector, tensor or pseudotensor. For such interactions, the dark matter-proton spin-independent scattering cross-section ($\sigma^p_{\rm SI}$) can be unambiguously related to the dark matter annihilation cross-section.

We will be interested in IVDM models which couple only to up and down quarks, since these provide conservative bounds. Couplings to all other quarks are isospin-invariant, and would result in a larger dark matter annihilation cross-section for fixed $\sigma^p_{\rm SI}$. We will only consider operators which yield spin-independent, velocity-independent scattering matrix elements. Furthermore, one will only obtain relevant bounds from Fermi data if the annihilation matrix element is s-wave. Given these choices, there are only three effective operators to consider:

$$\begin{aligned}
\mathcal{O}_D &= C^q_D \frac{1}{M_*^2} \bar{X}\gamma^\mu X \bar{q}\gamma_\mu q \\
\mathcal{O}_C &= C^q_C \frac{1}{M_*} X^* X \bar{q} q \\
\mathcal{O}_R &= C^q_R \frac{1}{M_*} X^2 \bar{q} q
\end{aligned} \tag{3}$$

where $\mathcal{O}_{D,C,R}$ are possible couplings if the dark matter (X) is a Dirac fermion, complex scalar or real scalar, respectively.[1] Here, $C^q_{D,C,R}$ are dimensionless couplings, M_* is an overall energy scale and $q = u, d$. The WIMPless model [26–28] exhibited in [13] as an example of IVDM was a real scalar coupling through $\mathcal{O}_R$.

The $\sigma^{p,n}_{\rm SI}$ can then be written as

$$\begin{aligned}
\sigma^{p,n(D)}_{\rm SI} &= \frac{\mu_p^2 f^2_{p,n}}{\pi M_*^4} \\
\sigma^{p,n(C)}_{\rm SI} &= \frac{\mu_p^2 f^2_{p,n}}{4\pi M_*^2 m_X^2} \\
\sigma^{p,n(R)}_{\rm SI} &= \frac{\mu_p^2 f^2_{p,n}}{\pi M_*^2 m_X^2}
\end{aligned} \tag{4}$$

where μ_p is the dark matter-proton reduced mass and the $f_{p,n}$ are coefficients parameterizing the coupling of dark matter to protons and neutrons, respectively. For $f_n/f_p \sim -0.7$, the constraints from XENON10/100 are maximally suppressed because of almost exact cancelation between proton and neutron interactions in the xenon target [12, 13]. Moreover, for this choice of f_n/f_p,

[1] Majorana fermions are not considered because there is no corresponding operator producing both s-wave annihilation and velocity-independent scattering. Also, it is useful to note that the most popular Majorana candidate, the neutralino in supersymmetry, is at least marginally inconsistent with the observations from CoGeNT, DAMA, and SIMPLE [25].

the regions favored by DAMA and CoGeNT are brought into alignment.

The $f_{p,n}$ are related to the coefficients $C^{u,d}$ by

$$f_p = C^u B_u^p + C^d B_d^p$$
$$f_n = C^u B_u^n + C^d B_d^n \quad (5)$$

where $B_{u,d}^{p,n}$ are the integrated nuclear form-factors [29]. When the dark matter is a scalar it couples through operator $\mathcal{O}_{C,R}$ to the scalar quark current, and the form factors are roughly given by $B_u^{p(scl.)} = B_d^{n(scl.)} \sim 6$ and $B_u^{n(scl.)} = B_d^{p(scl.)} \sim 4$. When the dark matter is a Dirac fermion it couples through operator $\mathcal{O}_D$ to the vector quark current, and the appropriate form factors are $B_u^{p(vec.)} = B_d^{n(vec.)} = 2$ and $B_u^{n(vec.)} = B_d^{p(vec.)} = 1$.

The annihilation cross-section arising from each effective operator can be written as

$$\langle \sigma_A^D v \rangle = \frac{3 m_X^2}{\pi M_*^4} (|C^u|^2 + |C^d|^2)$$
$$\langle \sigma_A^C v \rangle = \frac{3}{4\pi M_*^2} (|C^u|^2 + |C^d|^2)$$
$$\langle \sigma_A^R v \rangle = \frac{3}{\pi M_*^2} (|C^u|^2 + |C^d|^2) \quad (6)$$

If the dark matter is a Dirac fermion or complex scalar, we will assume that the dark matter particle and anti-particle number densities in Milky Way satellites are equal.

For any choice of f_n/f_p and choice of the interaction operator, one can use eqns. 4,5,6 to obtain constraints on $\sigma_{\rm SI}^p$ from the bounds in figure 1. These constraints are shown in figure 2 for $f_n/f_p \sim -0.7$, assuming dark matter interacting through $\mathcal{O}_C$ (if dark matter couples through $\mathcal{O}_R$ or $\mathcal{O}_D$, the bounds would be tighter by a factor of 2 or ~ 4, respectively). Also shown are the signal regions of DAMA [1] (3σ, assuming no channeling [30, 31]), CoGeNT [2] (90% CL) and CRESST [3] (2σ), along with 90% CL exclusion contours from XENON10 [4], XENON100 [5], CDMS [6, 7] and SIMPLE [8]. As we can see from this figure, the CoGeNT region of interest would be excluded by the Fermi data, under the assumptions made here.

The CoGeNT experiment has recently reported a preliminary analysis indicating that their experiment may have more surface area contamination than originally thought [32, 33]. The effect of this correction would be to shift the CoGeNT region of interest to slightly larger mass and slightly smaller $\sigma_{\rm SI}^p$, though the magnitude of the shift can only be determined by a complete analysis from the CoGeNT collaboration. This shift would serve to weaken constraints from Milky Way satellites.

Uncertainties from particle physics and astrophysics. There are a several ways in which the bounds from Fermi data can be weakened. For example, if the effective interaction operator is generated by the exchange

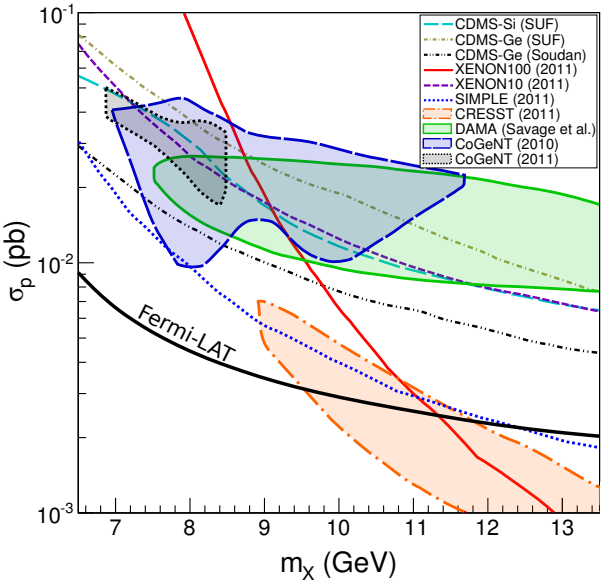

FIG. 2. Favored regions and exclusion contours in the (m_X, σ_p) plane for IVDM with $f_n/f_p = -0.7$. The solid black line is the bound from this analysis at 95% CL, assuming central values for the satellite density profile.

of a mediating particle with mass $m_\phi \sim 1$ GeV, then the momentum transfer during scattering interactions at any direct detection experiment ($\mathcal{O}(10$ keV$)$) would be much smaller than the mediator mass [34]. As a result, scattering interactions would still be described by an effective contact operator. However, the annihilation cross-section would receive an additional suppression of $(m_\phi/2m_X)^4 \sim 10^{-4} - 10^{-5}$. In this case, models with $\sigma_{\rm SI}^p$ which could match the CoGeNT data would be unconstrained by limits from dwarf spheroidals by $\sim 3-4$ orders of magnitude.

In addition, bounds from Fermi would be insignificant if dark matter interactions were mediated by an operator yielding velocity-independent spin-independent scattering, but p-wave suppressed annihilation. An example of such an operator would be $(1/M_*^2)\bar{X}X\bar{q}q$, in the case where the dark matter is a fermion. Another example would be $(1/M_*^2)X^*\partial_\mu X \bar{q}\gamma^\mu q$, if the dark matter is a complex scalar. Dark matter coupling through these operators would have an annihilation cross-section which is suppressed by v^2; the constraints from Fermi on $\sigma_{\rm SI}^p$ would thus be suppressed by more than 6 orders of magnitude. These models could potentially explain the low-mass data of DAMA, CoGeNT and XENON10/100, but would be unconstrained by the Fermi-LAT dwarf spheroidal search.

Both p-wave suppressed annihilation and light mediators would similarly weaken the bounds from anti-proton flux. In either case, the constraints from the anti-proton flux are suppressed by the same factor as the gamma-ray bounds, as discussed above. Such models matching

the CoGeNT, DAMA and XENON10/100 data would be unconstrained by bounds from BESS-Polar II.

The dark matter-proton scattering cross-section needed to match low-mass direct detection data can be shifted by other particle physics or astrophysics uncertainties, such as uncertainties in the nuclear form factor or in the dark matter velocity distribution near the earth. To normalize with all of the observations, here we have used the standard halo model to calculate the WIMP velocity distribution (e.g. [35]); variations from this model may affect the results presented, especially for high mass targets [36].

Complementary searches. There are interesting constraints on the annihilation of low-mass dark matter from WMAP-7 data [37, 38]. These constraints arise from the effect on standard recombination of the photons produced by dark matter annihilation. In the mass range we consider (assuming u/d-channel annihilation), the bounds which we obtain from dwarf spheroidals are a factor of ~ 5 tighter than those arising from WMAP-7 data. Note there are some systematic uncertainties in the WMAP-7 bounds regarding the effect of proton production on heating of the cosmic medium [38]. Again, these uncertainties are different from and independent of the uncertainties in dwarf spheroidal searches. Planck data is expected to significantly improve these CMB bounds.

There have been several recent studies of constraints on low-mass dark matter arising from the neutrino flux yielded by annihilation in the sun [11, 39–43]. But neutrino detectors cannot constrain dark matter which annihilates primarily to first generation quarks. The final state quarks hadronize, and these light hadrons typically lose energy and stop in the sun before decaying. They thus produce a neutrino spectrum far too soft to be distinguished from the atmospheric neutrino background.

The Fermi-LAT gamma-ray bounds are also complementary to recent constraints from collider monojet searches [44–48] on effective contact operators coupling dark matter to quarks. However, applying previous results to the case considered here is difficult, since they have typically assumed a dark matter coupling to all quarks. In particular, bounds in previous studies depend strongly on the existence of heavy quark operators, and are weakened considerably when only couplings to first generation quarks are present.

To address this issue, we provide simple bounds for $\sigma^p_{\rm SI}$ given couplings only to up and down quarks with $f_n/f_p = -0.7$. These bounds are based on an ATLAS monojet search using 1 fb^{-1} of data [49]. We present bounds for two possible selection cuts on $\not{E}_T$ and on the p_T of the leading jet: $p_T > 120$ GeV, $\not{E}_T > 120$ GeV and $p_T > 350$ GeV, $\not{E}_T > 300$ GeV. In addition to these selection cuts, the ATLAS study also used an intermediate cut of $\not{E}_T > 250$ GeV, $p_T > 220$ GeV. The bounds provided by this intermediate cut lie between those of the other two, and are not shown. For each choice of selection cuts, the ATLAS collaboration determined a bound on the $pp \to XXj$ cross-section attributable to new physics, based on a comparison of the number of observed events to the expected number of background events.

m_X	$\mathcal{O}_D$	$\mathcal{O}_C$	$\mathcal{O}_R$
4	0.00285	90.6	181
7	0.00320	35.4	70.3
10	0.00357	18.9	37.6
15	0.00370	9.1	18.2
20	0.00380	5.4	10.9

(a) $p_T > 120$ GeV, $\not{E}_T > 120$ GeV

m_X	$\mathcal{O}_D$	$\mathcal{O}_C$	$\mathcal{O}_R$
4	0.00079	10.8	21.6
7	0.00092	4.2	8.50
10	0.00097	2.3	4.51
15	0.00106	1.1	2.13
20	0.00107	0.62	1.24

(b) $p_T > 350$ GeV, $\not{E}_T > 300$ GeV

TABLE I. Upper bounds on $\sigma^p_{\rm SI}$ in pb from ATLAS monojet searches, assuming the listed cuts on the leading jet p_T and on the missing transverse energy. Masses are listed in GeV. The columns correspond to Dirac fermions, complex scalars, and real scalars respectively.

For IVDM models, we generated the production cross-section for each of the effective operators in eqn. 3 using MadGraph/MadEvent 5.1.3 [50]. The selection cuts were imposed at the parton level. According to the analysis of [47, 48, 51], approximately 40% of the events satisfying the cuts at parton level will satisfy the cuts once hadronization and detector effects are included. Accounting for this 40% selection efficiency, we determined upper bounds on $C^{u,d}_{C,R}/M_*$ for the scalar case and $C^{u,d}_D/M_*^2$ for the Dirac case. These translate directly into the upper bounds on $\sigma^p_{\rm SI}$ given in Table I for the two sets of missing energy and p_T cuts. Equivalent Tevatron bounds from CDF monojet searches [52] are weaker than the ATLAS bounds (assuming the $p_T > 120$ GeV, $\not{E}_T > 120$ GeV selection cut) by a factor of ~ 4. If dark matter is a real or complex scalar the monojet search sensitivity is significantly weaker than the sensitivity of Fermi-LAT and direct detection experiments. Only in the case of Dirac dark matter are collider bounds comparable to the Fermi-LAT constraint.

However, in the case of light mediators, collider bounds become significantly weaker. Assuming that the $\bar{q}q \to \bar{X}X$ process proceeds through the s-channel, the collider cross-section scales as $(p^2_\phi - m^2_\phi)^{-2}$. For light mediators we have $m_\phi \ll |p_\phi| > 2m_X$. This leads to a collider cross-section which is suppressed by at least $(2m_X)^{-4}$, instead of m_ϕ^{-4}. The corresponding rescaling of the direct detection bound relative to the contact operator case is at least $(2m_X/m_\phi)^4$, weakening the bound significantly [48]. If $m_\phi \sim 1$ GeV, the bound on $\sigma^p_{\rm SI}$ would be raised by a factor of $\sim 10^4 - 10^5$, placing relevant direct detection cross-sections for any species of dark matter well out of range of collider studies even at the LHC, at least in the conservative case of couplings only to light quarks and

through low-mass mediators.[2]

Conclusions. We have shown that Fermi-LAT gamma-ray searches of Milky Way satellites can constrain the cross-section for low-mass dark matter to annihilate to up or down-quarks. These constraints are tighter than for models with annihilation primarily to b-quarks or τ-leptons, due to the larger number of photons arising from annihilation to first-generation quarks. This is especially interesting in the case of isospin-violating dark matter, where destructive interference between up and down quark couplings imply an enhancement in the annihilation cross-section for models which can match the low-mass data of DAMA, CoGeNT and XENON10/100. In particular, IVDM models whose effective contact interactions yield s-wave annihilation are tightly constrained. Nevertheless, there are IVDM models which can evade these Fermi-LAT bounds and other constraints from indirect detection and collider searches. These IVDM models involve either low-mass mediators, or effective interaction operators which yield p-wave suppressed annihilation.

It is worth noting that microscopic dark matter models may involve interactions mediated by more than one effective operator. To understand constraints on such models from gamma-ray searches, one would need to know how the coefficients of the various interaction effective operators are correlated in any particular model.

In the case where dark matter annihilates to first generation quarks, the sensitivity of indirect search strategies depends on the spectrum of first generation quarks. The photon spectrum arising from the hadronization and decay of first generation quarks is peaked at low values of E_γ/m_X. Future searches using Milky Way satellites would thus greatly benefit in any reduction in the gamma-ray analysis threshold, E_{thr}.

Acknowledgments. We gratefully acknowledge S. Koushiappas and W. Shepherd for useful discussions, and Jonathan L. Feng for initial collaboration on this project. We also thank the Hawaii Open Supercomputing Center, and D. Hafner for facilitating our use of HOSC. JK and LES are grateful to Aspen Center for Physics, where part of this work was done, for their hospitality. JK is supported by DOE grant DE-FG02-04ER41291. DS is supported by NSF grant PHY0970173 and a UC Irvine Graduate Deans Dissertation Fellowship.

[1] R. Bernabei, *et al.*, Eur. Phys. J. **C67**, 39-49 (2010). [arXiv:1002.1028 [astro-ph.GA]].

[2] Note that for light mediators, the CDF monojet search [52] can place bounds which are tighter than the ATLAS search by a factor ~ 10 [53]. These bounds still do not constrain the IVDM models discussed here.

[2] C. E. Aalseth, *et al.*, Phys. Rev. Lett. **107**, 141301 (2011). [arXiv:1106.0650 [astro-ph.CO]].
[3] G. Angloher, *et al.*, [arXiv:1109.0702 [astro-ph.CO]].
[4] J. Angle *et al.*, Phys. Rev. Lett. **107**, 051301 (2011). [arXiv:1104.3088 [astro-ph.CO]].
[5] E. Aprile *et al.*, Phys. Rev. Lett. **107**, 131302 (2011). [arXiv:1104.2549 [astro-ph.CO]].
[6] D. S. Akerib *et al.*, Phys. Rev. D **82**, 122004 (2010) [arXiv:1010.4290 [astro-ph.CO]].
[7] Z. Ahmed *et al.*, Phys. Rev. Lett. **106**, 131302 (2011). [arXiv:1011.2482 [astro-ph.CO]].
[8] M. Felizardo, *et al.*, [arXiv:1106.3014 [astro-ph.CO]].
[9] A. Kurylov and M. Kamionkowski, Phys. Rev. D **69**, 063503 (2004) [arXiv:hep-ph/0307185];
[10] F. Giuliani, Phys. Rev. Lett. **95**, 101301 (2005) [arXiv:hep-ph/0504157].
[11] A. L. Fitzpatrick, D. Hooper and K. M. Zurek, Phys. Rev. D **81**, 115005 (2010) [arXiv:1003.0014 [hep-ph]].
[12] S. Chang, *et al.*, JCAP **1008**, 018 (2010). [arXiv:1004.0697 [hep-ph]].
[13] J. L. Feng, *et al.*, Phys. Lett. **B703**, 124-127 (2011). [arXiv:1102.4331 [hep-ph]].
[14] M. T. Frandsen, *et al.*, Phys. Rev. D **84**, 041301 (2011) [arXiv:1105.3734 [hep-ph]].
[15] J. M. Cline and A. R. Frey, Phys. Rev. D **84**, 075003 (2011) [arXiv:1108.1391 [hep-ph]]; J. M. Cline and A. R. Frey, arXiv:1109.4639 [hep-ph].
[16] J. Kopp, T. Schwetz and J. Zupan, arXiv:1110.2721 [hep-ph].
[17] The Fermi-LAT Collaboration, arXiv:1108.3546 [astro-ph.HE].
[18] A. Geringer-Sameth and S. M. Koushiappas, arXiv:1108.2914 [astro-ph.CO].
[19] M. L. Garde, *et al.*, [arXiv:1111.0320 [astro-ph.HE]].
[20] T. Sjostrand, S. Mrenna and P. Z. Skands, JHEP **0605**, 026 (2006) [hep-ph/0603175].
[21] K. Abe *et al.*, Phys. Rev. Lett. **108**, 051102 (2012) [arXiv:1107.6000 [astro-ph.HE]]; R. Kappl and M. W. Winkler, arXiv:1110.4376 [hep-ph].
[22] Q. -H. Cao, I. Low and G. Shaughnessy, Phys. Lett. B **691**, 73 (2010) [arXiv:0912.4510 [hep-ph]].
[23] J. Lavalle, Phys. Rev. D **82**, 081302 (2010) [arXiv:1007.5253 [astro-ph.HE]].
[24] C. Evoli, I. Cholis, D. Grasso, L. Maccione and P. Ullio, arXiv:1108.0664 [astro-ph.HE].
[25] E. Kuflik, A. Pierce and K. M. Zurek, Phys. Rev. D **81**, 111701 (2010) [arXiv:1003.0682 [hep-ph]].
[26] J. L. Feng and J. Kumar, Phys. Rev. Lett. **101**, 231301 (2008) [arXiv:0803.4196 [hep-ph]].
[27] J. L. Feng, J. Kumar and L. E. Strigari, Phys. Lett. B **670**, 37 (2008) [arXiv:0806.3746 [hep-ph]].
[28] J. L. Feng, H. Tu and H. -B. Yu, JCAP **0810**, 043 (2008) [arXiv:0808.2318 [hep-ph]].
[29] J. R. Ellis, *et al.*, Eur. Phys. J. C **24**, 311 (2002) [astro-ph/0110225]; G. Belanger, *et al.*, Comput. Phys. Commun. **180**, 747 (2009) [arXiv:0803.2360 [hep-ph]].
[30] C. Savage, *et al.*, JCAP **0904**, 010 (2009) [arXiv:0808.3607 [astro-ph]].
[31] C. Savage, *et al.*, Phys. Rev. D **83**, 055002 (2011) [arXiv:1006.0972 [astro-ph.CO]].
[32] Talk by J. Collar, TAUP 2011 Workshop, Munich, Germany, Sep. 5-9, 2011.
[33] C. Kelso, D. Hooper and M. R. Buckley, arXiv:1110.5338 [astro-ph.CO].

[34] N. Fornengo, P. Panci and M. Regis, arXiv:1108.4661 [hep-ph].
[35] C. McCabe, Phys. Rev. D **82**, 023530 (2010) [arXiv:1005.0579 [hep-ph]].
[36] M. Lisanti, *et al.*, Phys. Rev. D **83**, 023519 (2011) [arXiv:1010.4300 [astro-ph.CO]].
[37] G. Hutsi, *et al.*, arXiv:1103.2766 [astro-ph.CO].
[38] S. Galli, *et al.*, Phys. Rev. D **84**, 027302 (2011) [arXiv:1106.1528 [astro-ph.CO]].
[39] D. Hooper, *et al.*, Phys. Rev. D **79**, 015010 (2009) [arXiv:0808.2464 [hep-ph]].
[40] J. L. Feng, *et al.*, JCAP **0901**, 032 (2009) [arXiv:0808.4151 [hep-ph]].
[41] J. Kumar, J. G. Learned and S. Smith, Phys. Rev. D **80**, 113002 (2009) [arXiv:0908.1768 [hep-ph]].
[42] J. Kumar, *et al.*, Phys. Rev. D **84**, 036007 (2011) [arXiv:1103.3270 [hep-ph]].
[43] S. -L. Chen and Y. Zhang, Phys. Rev. D **84**, 031301 (2011) [arXiv:1106.4044 [hep-ph]].
[44] J. L. Feng, S. Su, F. Takayama, Phys. Rev. Lett. **96**, 151802 (2006). [hep-ph/0503117].
[45] J. Goodman, *et al.*, Phys. Lett. **B695**, 185-188 (2011). [arXiv:1005.1286 [hep-ph]].
[46] A. Rajaraman, *et al.*, [arXiv:1108.1196 [hep-ph]].
[47] J. Goodman, *et al.*, Phys. Rev. **D82**, 116010 (2010). [arXiv:1008.1783 [hep-ph]].
[48] J. Goodman, W. Shepherd, [arXiv:1111.2359 [hep-ph]].
[49] ATLAS Collaboration, ATLAS-CONF-2011-096.
[50] J. Alwall, M. Herquet, F. Maltoni, O. Mattelaer and T. Stelzer, JHEP **1106**, 128 (2011) [arXiv:1106.0522 [hep-ph]].
[51] Will Shepherd, private discussions.
[52] http://www-cdf.fnal.gov/physics/exotic/r2a/20070322.monojet/public/ykk.html
[53] A. Friedland, M. L. Graesser, I. M. Shoemaker and L. Vecchi, arXiv:1111.5331 [hep-ph].